

---

# Relating cell proliferation to *in vivo* bone formation in porous Ca/P scaffolds

---

Steven M. van Gaalen,<sup>1</sup> Joost D. de Bruijn,<sup>2</sup> Clayton E. Wilson,<sup>3</sup> Clemens A. van Blitterswijk,<sup>3</sup> Abraham J. Verbout,<sup>1</sup> Jacqueline Alblas,<sup>1</sup> Wouter J. A. Dhert<sup>1,4</sup>

<sup>1</sup>Department of Orthopaedics, University Medical Center Utrecht, P.O. Box 85500, 3508 GA Utrecht, The Netherlands

<sup>2</sup>The Department of Materials, Queen Mary, University of London, Mile End Road, London E1 4NS, United Kingdom

<sup>3</sup>Department of Tissue Regeneration, University of Twente, P.O. Box 217, 7500 AE, Enschede, The Netherlands

<sup>4</sup>Departments of Companion Animals and Equine Sciences, Faculty of Veterinary Medicine, Utrecht University, The Netherlands

Received 26 May 2008; revised 14 September 2008; accepted 16 October 2008

Published online 2 February 2009 in Wiley InterScience (www.interscience.wiley.com). DOI: 10.1002/jbm.a.32380

**Abstract:** Most current methods for cell monitoring on 3D porous scaffolds involve end-stage investigation of scaffolds. Repeated measurements on scaffolds, without disturbing cell vitality and proliferation, are needed to relate *in vitro* to *in vivo* data. Alamar Blue™ was used for this purpose. Two different Ca/P scaffolds were studied, using rat BMSCs with three different seeding densities [ $2.5 \times 10^4$  (SD1),  $2.5 \times 10^5$  (SD2),  $2.5 \times 10^6$  (SD3) cells]. Alamar Blue™ readings were done on days 1, 3, 5 and 7. After 7 days all 96 scaffolds ( $n = 16$ ) were implanted in 16 mice for 4 weeks. Bone histomorphometry was performed. For both scaffolds, seeding efficiencies were highest with SD1 and SD2, cell

proliferation was optimal in SD1, whereas SD3 resulted in an initial drop in vital cell number in the first 3 days. *In vivo*, upscaling from SD1 to SD2 lead to significantly more bone contact% in both scaffolds. Alamar Blue™ was shown to be a valuable tool in relating *in vitro* to *in vivo* data. Cell proliferation may differ depending on seeding density and scaffold type used. Seeding more cells may not necessarily result in more *in vivo* bone contact%. © 2009 Wiley Periodicals, Inc. J Biomed Mater Res 92A: 303–310, 2010

**Key words:** bone; tissue engineering; scaffold; cell quantification; histomorphometry

---

## INTRODUCTION

The *in vivo* success of bone formation by seeded osteoprogenitor cells (OPCs) on a scaffold material is subject to a certain number of variable *in vitro* factors. Several of these factors are known. Culture medium additives for species-specific bone marrow cell cultures are an example of these *in vitro* factors affecting the *in vivo* bone formation. Several of these culture medium additives are known based on optimized cell cultures over the years in different species such as rats,<sup>1</sup> mice,<sup>2</sup> rabbits,<sup>3</sup> goats<sup>4</sup> and humans.<sup>5</sup> Another example is seeding density. Used primarily in 2D cell cultures, this is related to the amount of cell doublings needed to obtain sufficient cell numbers for the seeding experiments under investigation. Effects on *in vitro* cell behavior using different seeding den-

sities in both the primary and subsequent passages have been found. Purpura et al. showed for rat OPCs an increase in Colony Forming Unit-Osteoblast (CFU-O) number when increased seeding densities were used in the primary passage.<sup>6</sup> Seeding density effects in subsequent passage numbers is also well documented for human cells. Some found a positive effect of increasing seeding density in subsequent passage numbers on the *in vitro* extracellular matrix mineral deposition using human OPCs.<sup>5</sup> Others showed that just 100 cells/cm<sup>2</sup> were found to be optimal in cell proliferation in 2D culture conditions, leaving the *in vivo* osteogenic potential unaffected when similar seeding densities were used upon 3D scaffold seeding prior to *in vivo* implantation.<sup>7</sup>

Seeding cells on 3D scaffolds (instead of the 2D culture plates) introduces additional factors affecting cell behavior in the final stage prior to implantation that could overrule the cell proliferation and differentiation features observed in the 2D culture conditions prior to seeding. It is likely that an optimal scaffold-specific seeding density will exist for scaffolds of different types and structures, and for different species. This optimum may be different for fac-

Correspondence to: S. M. van Gaalen; e-mail: s.m.gaalens@umcutrecht.nl

Contract grant sponsor: The Netherlands Technology Foundation; contract grant number: UGN.4966

tors such as seeding efficiency, cell proliferation and cell differentiation which may all affect *in vivo* bone formation to a certain extent. Data concerning these parameters on 3D scaffold seeding were shown for instance in rabbit OPCs on hydroxyapatite scaffolds,<sup>8</sup> rat OPCs on polymer scaffolds,<sup>9</sup> rat calvarial cells on polymers,<sup>10</sup> human OPCs on collagen scaffolds<sup>11</sup> or goat OPCs on hydroxyapatite scaffolds.<sup>12</sup> Unfortunately the participation of the examined scaffolds for *in vivo* bone formation was never feasible once *in vitro* testing was performed since all of these tests involved terminal investigation of the scaffolds. This calls for less invasive methods for cell proliferation studies on 3D porous scaffolds. The introduction of the fluorescent dye alamarBlue™ (aB) has offered new opportunities in 3D cell-seeding research<sup>12–14</sup> allowing the continued study participation of the scaffolds for *in vivo* use. aB is an oxidation-reduction indicator that yields a color change and fluorescent signal upon a change in metabolic activity. The assay can be applied to determine cell vitality and proliferation in an easy to use and nontoxic way, allowing the same cells to remain vital within the experimental settings in contrast to assays such as MTT<sup>15</sup> or Cyquant (DNA)<sup>16</sup> assays where cells are terminally destructed for quantification purposes. One of the drawbacks of the aB system is, however, its diffusion dependency, making the permeability of especially the 3D structures potentially affect the results. Overall the aB assay, analogous to the alternative assays, should be considered as a semi-quantitative rather than a quantitative assay when measuring cell numbers in 3D scaffolds.

The purpose of this study was to monitor rat OPC proliferation behavior on two geometrically different types of hydroxyapatite scaffolds *in vitro*, in response to three different seeding densities with the use of this aB assay. Subsequent *in vivo* bone formation was related to *in vitro* cell proliferation using histomorphometry data obtained after subcutaneous implantation of the same scaffolds in nude mice.

## MATERIALS AND METHODS

### Animals and study design

A total of three young syngeneic Fisher rats (100–120 g, F344N:Hsd, Harlan, The Netherlands) and 16 mice (10–12 weeks of age, HsdCpb:NMRI-nu, Harlan, The Netherlands) were used for the current experiment, after approval was obtained from the local animal care committee. Third passage cells were obtained after pooling rat femoral bone marrow that was flushed from the marrow cavities using a syringe and needle. Cells were used for static seeding on rapid prototyped hydroxyapatite, rectangular-shaped scaffolds (group A)<sup>17</sup> and on conventional granu-

lar-shaped porous hydroxyapatite scaffolds (group B).<sup>18</sup> Three different seeding densities (SD) were used for each group of scaffolds: (SD1)  $2.5 \times 10^4$ , (SD2)  $2.5 \times 10^5$  and (SD3)  $2.5 \times 10^6$  cells per scaffold, corresponding to  $1 \times 10^3$ ,  $1 \times 10^4$ , and  $1 \times 10^5$  cells per  $\text{mm}^3$  of scaffold A and an estimated  $1.6 \times 10^3$ ,  $1.6 \times 10^4$ , and  $1.6 \times 10^5$  cells per  $\text{mm}^3$  of scaffold B (based on average weight of the scaffolds and mercury intrusion data<sup>19</sup>). During the 7 days of seeding, aB readings were performed on days 1, 3, 5, and 7. On day 7, all scaffolds were implanted subcutaneously in nude mice. Each mouse was implanted with all three seeding densities for both group A and group B scaffolds ( $n=16$ ). This accounts for the total of 96 scaffolds implanted for the *in vivo* part of this study. In each mouse, scaffold position was randomized with three scaffolds of the same group subcutaneously on each side of the midline. Outcome parameters in this study were vital cell numbers on days 1, 3, 5, and 7 in the *in vitro* part and bone-scaffold contact length percentage for the *in vivo* part based on histomorphometry readings.

### Scaffolds [Figure 1(A–E)]

#### Group A scaffolds (rapid prototyping)

Commercially available hydroxyapatite (HA) powder (Merck Eurolab BV, The Netherlands) was used for the fabrication of these scaffolds. XRD (XRD; Miniflex, Rigaku, Japan) was used to determine crystallinity, chemical composition was determined by Fourier transformed infrared spectroscopy (FT-IR, Spectrum 1000, PerkinElmer) and scaffold dimensions were studied using Scanning Electron Microscopy (SEM) (Philips XL 30; ESEM-FEG, The Netherlands). The calculated porosity of the scaffolds (based on SEM two-dimensional data) was  $52\% \pm 2\%$ . The designed surface area was  $2.5 \text{ cm}^2$ . Pore sizes were  $(286 \pm 15) \times (280 \pm 16) \mu\text{m}$  in the  $x$ - $y$  plane,  $(352 \pm 28) \times (339 \pm 17) \mu\text{m}$  in the  $x$ - $z$  plane and  $(394 \pm 24) \times (376 \pm 30) \mu\text{m}$  in the  $y$ - $z$  plane. For detailed information on XRD patterns we refer to previous work.<sup>17</sup> The scaffolds were steam-sterilized for 20 min at  $121^\circ\text{C}$ .

#### Group B scaffolds (conventional scaffolds)

For the preparation of these scaffolds the same commercially available HA powder was used as in group A. Similar studies were performed on these scaffolds using XRD, FT-IR, and SEM as for group A. The average porosity of the scaffolds was  $67\% \pm 3\%$  as determined by mercury intrusion.<sup>19</sup> The surface area of this scaffold was unknown. The pores had an average pore size of  $436 \mu\text{m}$  and a range of  $300\text{--}800 \mu\text{m}$ . For further details we refer to previous work.<sup>18</sup> The granules were steam-sterilized for 20 min at  $121^\circ\text{C}$ .

### *In vitro* scaffold seeding

Bone marrow cells from the rats were harvested and culture expanded *in vitro* according to standard condi-

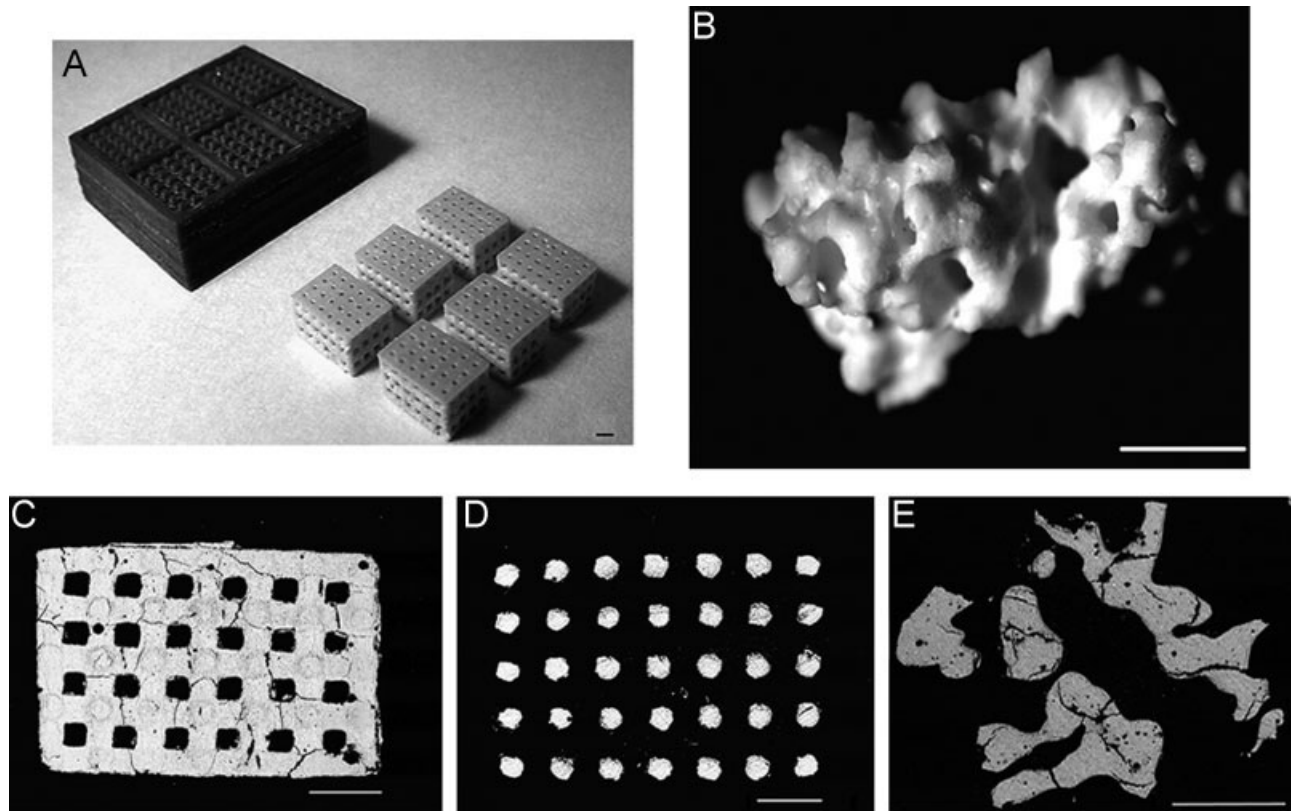


**Figure 1.** A: Macroscopic image of scaffolds from group A, fabricated using the technique of rapid prototyping with an open pore structure and regular shape with known surface area. B: Macroscopic image of a scaffold from group B, a granular shape with unknown scaffold surface area. C, D: Microscopic images (SEM-backscattering technique) with details from group A scaffolds with C showing the open, fully connected, pore structure in contrast to D showing a horizontal section through the area containing the back-bone of the same scaffold. The scaffold structure is white, the pores are black. E: Microscopic detail (SEM-backscattering technique) of a scaffold in group B. The scaffold structures are white, the pores are black. Scale bars represent 1 mm.

tions.<sup>18</sup> At the end of passage two, when cells were near confluency, a cell suspension of  $5 \times 10^7$  cells per ml was created to seed 50  $\mu\text{L}$  per scaffold in the group of  $2.5 \times 10^6$  (=SD3) cells per scaffold and subsequent dilutions were performed to create  $2.5 \times 10^5$  (=SD2) and  $2.5 \times 10^4$  (=SD1) cells per scaffold. The cell densities per  $\text{mm}^3$  of scaffold were calculated based on the 52.3% porosity in scaffold group A with an average block volume of  $47.3 \pm 1.1 \text{ mm}^3$  per sample (= 25  $\text{mm}^3$  of scaffold volume),<sup>17</sup> leading to  $1 \times 10^3$ ,  $1 \times 10^4$ , and  $1 \times 10^5$  cells/ $\text{mm}^3$  of scaffold A. For scaffold group B the same procedure was applied. With the same bulk material for the fabrication of these scaffolds, presuming a similar amount of shrinkage in both scaffold groups, the true density of scaffold A ( $71.2 \pm 4.2 \text{ mg}$  (=average weight)/ $47.3 \pm 1.1 \text{ mm}^3 = 1.5 \text{ mg}/\text{mm}^3$ ) was applied to calculate the scaffold volume of scaffold B. In scaffold B, with a 67% porosity, the same seeding procedure lead to an estimated  $1.6 \times 10^3$ ,  $1.6 \times 10^4$ , and  $1.6 \times 10^5$  cells per  $\text{mm}^3$ . For this purpose, the cell droplets of 50  $\mu\text{L}$  were immediately resuspended throughout each scaffold and incubated for 2 h in a 25-well non-culture plate (Greiner, The Netherlands), prior to adding fresh culture medium to each scaffold. On days 1, 3, 5, and 7 all scaffolds were transferred to new plates for the

aB assay to avoid any potential metabolic effect on the aB assay of cells present in the culture dish. For the assay, a 10% aB culture medium solution was made simply by adding 10 volume percent of aB (Biosource International) to fully supplemented rat culture medium. The added volume of aB medium (37°C) was 3 mL per scaffold to each well for an incubation period of 2 h on a *x-y-z* shaking platform at low speed. After 2 h, 200  $\mu\text{L}$  duplicate medium samples were obtained from each well and transferred to the appropriate microwell plates. A minimum of six blanks were included for each plate. The plate was then covered with aluminum foil and placed on the counter for 1 h to equilibrate with room temperature. The plate was subsequently analyzed by a fluorometer (Perkin-Elmer) with the settings as prescribed by the manufacturer of the aB assay and as performed previously.<sup>12</sup> Fluorescence values were related to standard curves obtained with cells from the same study and passage number that were plated in 6-well culture plates. Linear standard curves from these cells were derived in quadruplets based on initial plating densities of  $5 \times 10^4$ ,  $1 \times 10^5$ ,  $2.5 \times 10^5$ ,  $5 \times 10^5$ , and  $7.5 \times 10^5$  cells per well. The amount of cells present on the scaffolds on day 1 in comparison to the amount of cells seeded was considered as our seeding efficiency. Population doublings



**TABLE I**  
**Overview of the Seeding Efficiency, Population Doublings and Cell Numbers on the Scaffolds on the Day of Implantation (day 7) From the *In Vitro* Part of the Study Based on the aB Readings**

	Group A			Group B		
	SD1	SD2	SD3	SD1	SD2	SD3
Seeding efficiency (%)	28.3 ± 5.9	26.6 ± 4.0	5.9 ± 0.7	15.8 ± 4.3	17.6 ± 6.5	5.2 ± 1.0
Population doublings	3.4	1.2	-0.3	4.3	1.2	-0.5
Cell No Day Of Implant ( $\times 10^4$ Cells)	7.3 ± 1.5	15.1 ± 1.3	12.1 ± 1.6	7.9 ± 1.2	10.4 ± 1.5	9.3 ± 2.3

Numbers are indicated  $\pm$  standard deviations. Negative numbers in population doublings indicate a decrease in total cell number from day 1 to day 7. Group A and B indicate scaffold group A and B respectively. SD indicates seeding density. For statistical comparisons in cell numbers see also *in vitro* results.

in the different seeding density groups for both scaffolds were calculated based on the following formula: population doubling =  $(\log N_t - \log N_0) / \log 2.0$  with  $N_t$  representing the cells on day 7 and  $N_0$  representing the cells on day 1.<sup>20</sup>

In addition to the cell proliferation assay using aB, a few scaffolds from both groups were used for staining purposes on day 7 using a cell-attachment staining solution of methylene blue, a staining solution for nonvital cells [Trypan Blue (TB)] and a vitality staining using MTT.<sup>18</sup>

### ***In vivo* sample processing and histomorphometry**

After 6 weeks, the mice were killed by cervical dislocation and explanted samples were fixed in 1.5% glutaraldehyde, dehydrated by ethanol series and embedded in polymethylmethacrylate. Semi-thin sections (10  $\mu$ m) were made with a Leica sawing microtome, stained with methylene blue and basic fuchsin for routine histology<sup>21</sup> and histomorphometry. All scaffolds were fully sectioned with scaffold type A always sectioned in the *x-y* plane.<sup>17</sup> Samples were first evaluated for general tissue response and bone formation using a light microscope (E600 Nikon, Japan). The mid-sections for both scaffold groups were carbon-sputter-coated and evaluated using a SEM backscattering technique. Digital images (75 dpi) were loaded into a PC running the KS400 program (Zeiss, Oberkochen, Germany).

All implants were analyzed for bone scaffold contact length percentage (Cont.% = percentage of total available scaffold contact length occupied by the contact with the newly formed bone).<sup>22</sup> In standard nomenclature<sup>23</sup> this could be formulated as:

$$\begin{aligned} \text{Cont.\%} &= \text{B.BCP.Bd\%} \\ &= \frac{[\text{BCP.Pm in contact with B.pm}]}{[\text{BCP.Pm total}]} \times 100\% \end{aligned}$$

where Bd = boundary, B = Bone, BCP = BCP scaffold and Pm = perimeter.

Based on the surface-related process of de novo bone formation in tissue engineered scaffolds the bone scaffold contact length percentage is considered more accurate as compared to the bone per pore area percentage since it

allows for structure-independent comparison of bone formation within scaffolds in 2D histology sections.<sup>22</sup>

### **Statistics**

SPSS 10 was used for statistical analysis. *In vitro* cell proliferation data (growth curves) for the *in vivo* implants ( $n = 16$  for each seeding density in each scaffold group, in total 96 scaffolds) were analyzed overall using a Repeated Measures Test. Cell number comparisons between different seeding densities for the *in vitro* aB analysis were compared using a one-way ANOVA. *In vivo* histomorphometry data were analyzed using a (nonparametric) Friedman and Wilcoxon test for related samples, since these data were not normally distributed. All comparisons between different seeding densities were Bonferroni corrected. No statistical comparisons were made between the *in vitro* and *in vivo* data of the two scaffold groups since the differences in scaffold structures between group A and B are most likely to influence both cell seeding behavior and aB exposure in different ways. Only comparisons within each group can suggest potential differences in effects between the three seeding densities. The level of significance was kept at  $p \leq 0.05$ .

## **RESULTS**

### ***In vitro***

Table I shows the seeding efficiency results for both scaffolds. For both scaffold groups, SD3 had the lowest seeding efficiency. Cell proliferation (Fig. 2): cell numbers for SD1 and SD2 in both groups showed an increase between days 1 and 7 with SD2 in group B reaching a plateau phase between days 5 and 7. SD3 showed an initial decline in cell number between days 1 and 5 followed by an inclination in cell numbers for both scaffold groups.

Overall, population doublings on the scaffolds in this study were highest in the lower seeding density (SD1) and negative in the highest seeding density (SD3) used for both scaffold type groups (Table I).

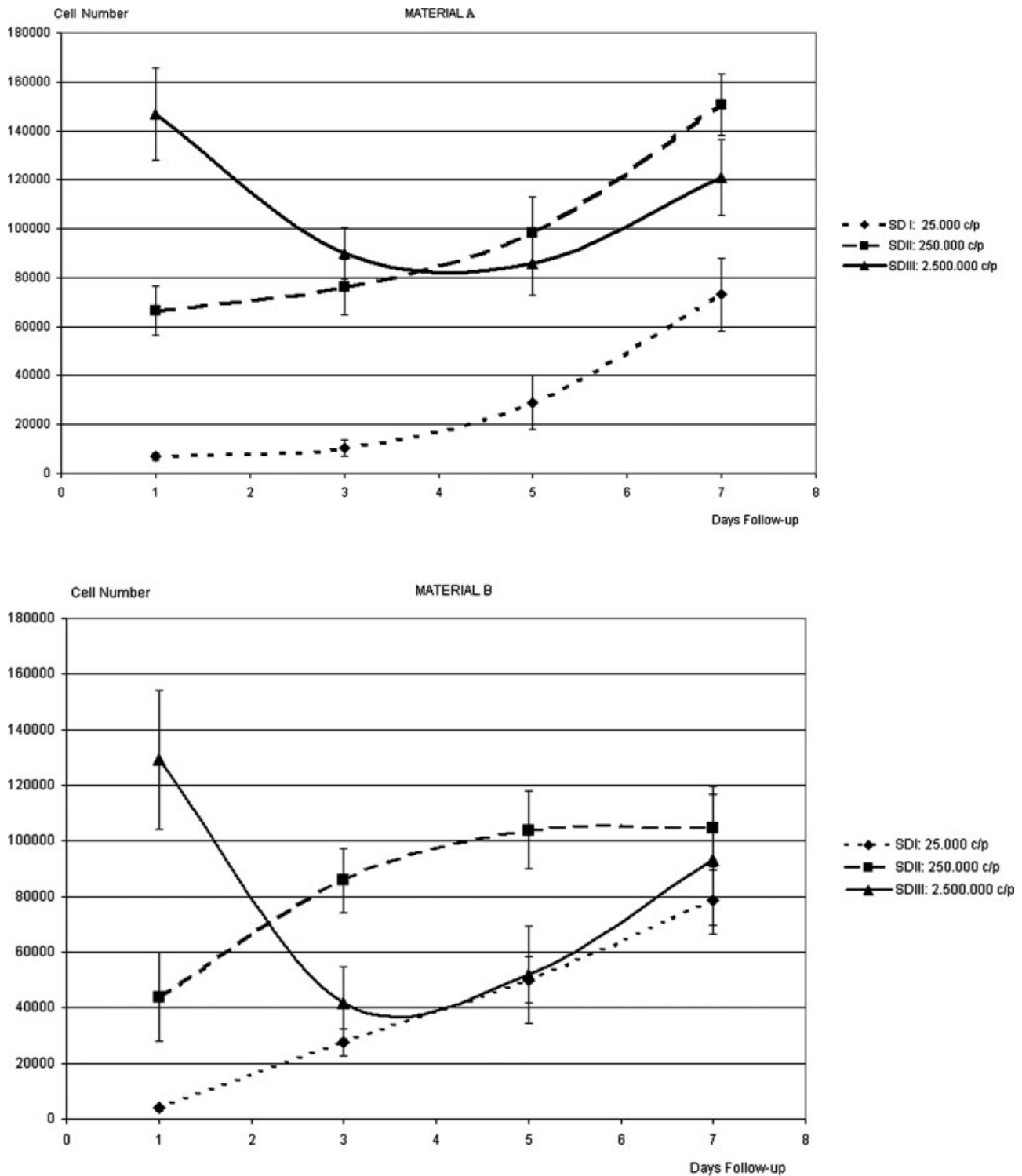


**Figure 2.** Cell numbers based on repeated aB readings on the same group of scaffolds ( $n = 16$ ) on days 1, 3, 5, and 7 that were used for *in vivo* implantation on day 7. Lines are extrapolations of the data obtained on days 1, 3, 5, and 7. Results are given as the mean  $\pm$  standard deviations. SDI, II, and III indicate seeding densities 1, 2, and 3. C/p indicates the number of cells per scaffold.

On the day of implantation, in scaffold group A, the largest number of cells on the scaffolds were present with SD2, followed by SD3 and SD1 ( $p < 0.001$  for all). Scaffold group B on the day of im-

plantation had the largest number of cells on scaffolds present with SD2, which was significantly more than SD1 ( $p < 0.001$ ) but not different from SD3 ( $p = 0.07$ ).

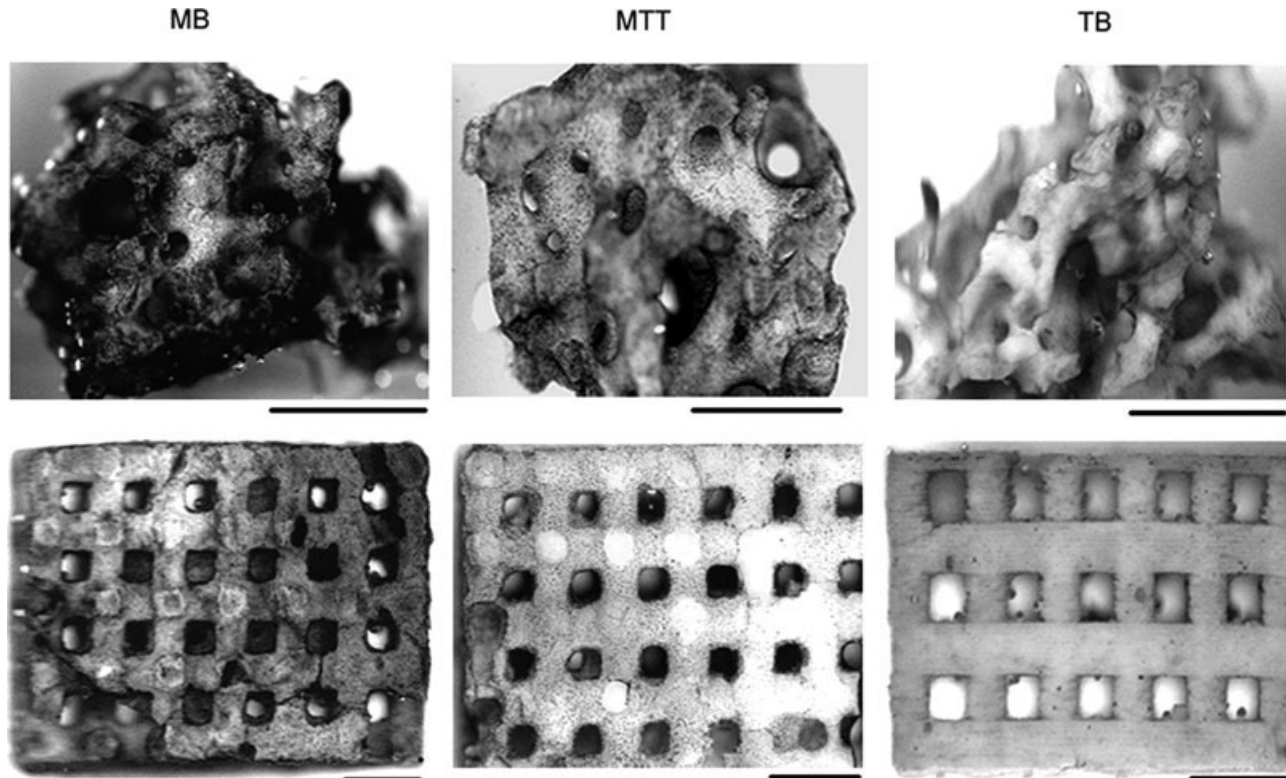


**Figure 3.** Methylene blue (MB) staining for cell attachment, MTT staining for cell vitality and Trypan Blue (TB) staining for nonvital cells on scaffolds from groups A (bottom row) and B (top row) for SD1. Note that few cells are stained with TB. Scale bars represent 1 mm.

### *In vitro* scaffold staining

Figure 3 shows images from group A and group B scaffolds seeded with SD1 for methylene blue (MB) staining on cell attachment, MTT staining on cell vitality and Trypan Blue (TB) staining for nonliving cells. MB and MTT images on both types of scaffolds indicate that the majority of the attached cells are vital. This is confirmed by the low amount of TB-positive cells. SD2 and SD3 scaffolds (data not shown) contain more confluent layers of attached and vital cells with only a modest increase in the number of nonvital cells on the TB staining images.

### *In vivo*

All the implanted mice survived the end of the study and remained in good health. On the day of explantation, all scaffolds appeared to be well incorporated into the subcutaneous host tissue, without fixation to the underlying fascia of the paraspinal musculature. Figure 4 shows an example of a backscatter scanning electron micrograph representing optimal bone formation for both groups. In group A, with SD1 no bone was formed in any of the mice (Table II). With SD2 in 7/16 mice bone formation

occurred in the scaffolds with an average bone-scaffold contact of  $1.6\% \pm 3.4\%$  (Table II). With SD3 in 11/16 mice bone in the scaffolds was observed with an average bone-scaffold contact of  $3.1\% \pm 7.4\%$ . SD2 and SD3 both showed a significant difference as compared to SD1 ( $p = 0.02$  and  $p = 0.003$  respectively), SD2 and SD3 were not significantly different ( $p = 0.6$ ). In group B, with SD1 in 3/16 mice bone was formed in the scaffolds with an average of  $0.3\% \pm 0.8\%$  bone-scaffold contact. Using SD2, in all (16/16) mice bone formation occurred in the scaffolds with an average of  $11.0\% \pm 10.3\%$  bone-scaffold contact. With SD3, in 13/16 mice bone was observed with  $5.3\% \pm 7.4\%$  bone-scaffold contact. Again, SD2 and SD3 both showed a significant difference when compared to SD1 ( $p < 0.001$  and  $p = 0.002$  respectively), however, SD2 and SD3 were not significantly different ( $p = 0.07$ ).

## DISCUSSION

Relating *in vitro* cell proliferation data to *in vivo* bone formation in an ectopic mouse model was shown to be feasible using the aB assay. Sequential 10-fold increases in the initial number of seeded cells on two geometrically different Ca/P scaffolds did

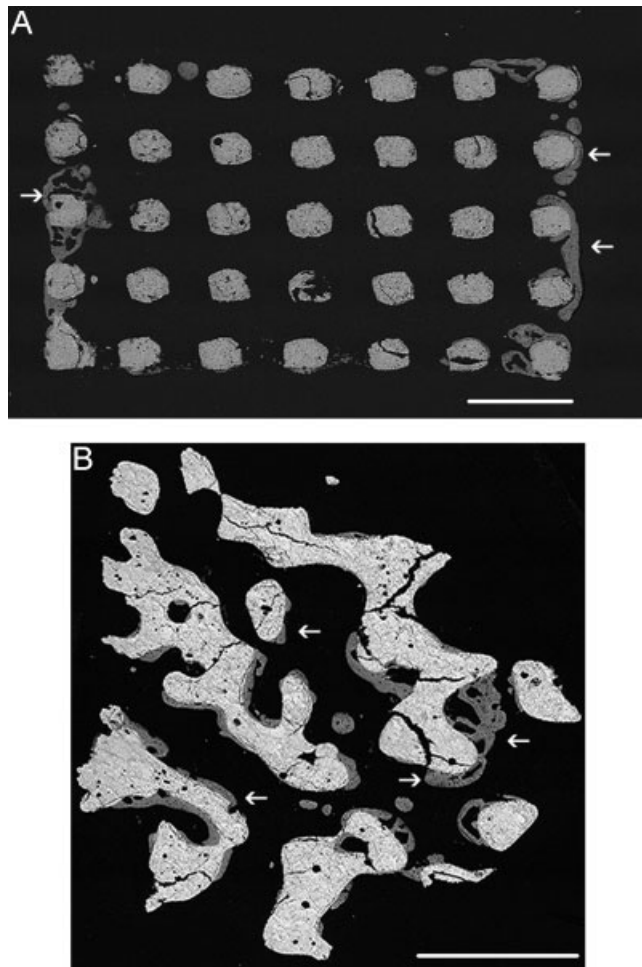


**Figure 4.** Backscattering images of mid-sections for scaffolds in group A (A) and group B (B). Both images are representative of the more optimal results of bone formed in these scaffolds after 6 weeks of *in vivo* implantation (examples represent SD3 for scaffold group A and SD2 for scaffold group B). White arrows indicate new bone formation on the scaffolds. Scale bars represent 1 mm.

not result in a steady increase in bone formation. Therefore, seeding more cells does not automatically relate to more bone formation. However, seeding SD1 for 7 days in this study was shown to be subop-

timal for both groups when both the bone score in mice and the contact length% are concerned. Further increases from SD2 to SD3 did not differ significantly within these parameters either. Looking at the results for scaffold group A one could speculate that a more favorable seeding technique (without an initial drop in vital cell numbers for SD3) could result in more vital cells per scaffold on day 7 and perhaps more optimal bone formation in this seeding density group. For scaffold group B it could be speculated that this optimum was already reached with SD2 since aB readings showed that no more than  $\approx 10.5 \times 10^4$  cells could be hosted on average on these scaffolds (Figure 2). Whether the time of constant cell numbers between days 5 and 7, which could indicate a state of "confluence" on these scaffolds, was of any influence on the optimal results in this seeding density group can not be concluded at this moment. Cell confluence in osteoblastic 2D cultures is directly related to a conversion from cell growth to cell differentiation with concomitant extracellular matrix deposition.<sup>24</sup> Cell characterization such as an increase in the alkaline phosphatase (ALP) activity or bone morphogenetic protein (BMP) production, could help to resolve this issue. If cell confluence on the scaffolds would be an important factor in relation to bone formation, optimization of seeding techniques (preventing an initial drop in cell number such as observed with SD3) and establishing an early scaffold cell confluence could be crucial.

The use of alamarBlue on rat BMCs has permitted us to compare between *in vitro* cell behavior in 3D scaffolds and *in vivo* bone formation on these same scaffolds. The ability to continue with a specific scaffold in a "repeated measures" method for cell quantification purposes and to apply this scaffold for subsequent *in vivo* implantation makes this method a strong alternative in comparison to the "terminal" use of scaffolds with, for example, MTT<sup>15</sup> or Cyquant.<sup>16</sup> These methods necessitate comparisons between groups of different scaffolds with subsequent risks in losing statistical power. Limitations to the aB assay are mainly found in the semi-quantita-

**TABLE II**  
The In Vivo Bone Score in Mice Indicates the Number of Mice Showing Bone in the Specific Seeding Density for Both Material Groups A and B

	Group A			Group B		
	SD1	SD2	SD3	SD1	SD2	SD3
Bone score in mice	0/16	7/16	11/16	3/16	16/16	13/16
Contact length(%)	$0.0 \pm 0.0^a$	$1.6 \pm 3.4^b$	$3.1 \pm 7.4^c$	$0.3 \pm 0.8^d$	$11.0 \pm 10.3^e$	$5.3 \pm 7.4^f$

Only SD2 in group B showed bone in all of the 16 mice. The contact length % indicates the amount of bone-scaffold contact length as a percentage of the total available scaffold contact length. Standard deviations are included for the contact length %. Statistical significant differences between the different seeding densities in each material group are here indicated in bold with their individual *p* values: Group A: **a-b** = 0.02; **a-c** = 0.003; **b-c** = 0.6 Group B: **d-e** < 0.001; **d-f** = 0.002; **e-f** = 0.07.



tive nature of the assay (comparing cell numbers in 3D structures to standard curves derived from 2D culture plates) and the dependency on the ease or difficulty of diffusion of the aB medium into the metabolically active cells. It can be speculated that the latter is influenced by scaffold geometry such as pore size, interconnectivity of the pores and fenestration size.<sup>19</sup> These items can be circumvented by avoiding comparisons between different types of scaffolds. Whether the penetration of the aB medium remains constant with increasing (calcifying) ECM formation in confluent cell layers on the scaffolds is unknown. This factor should be further studied and until then be considered as a potential bias in the comparisons between different seeding densities in this study, especially at later time points during culture.

In conclusion, scaffold structure and *in vitro* cell behavior (such as seeding efficiency and cell proliferation) can not be considered as two separate entities when the effects on *in vivo* bone formation are concerned. AlamarBlue was shown to be a valuable tool in the study on cell proliferation on our 3D constructs.

## References

- Maniopoulos C, Sodek J, Melcher AH. Bone formation in vitro by stromal cells obtained from bone marrow of young adult rats. *Cell Tissue Res* 1988;254:317–330.
- Franceschi RT, Iyer BS, Cui Y. Effects of ascorbic acid on collagen matrix formation and osteoblast differentiation in murine MC3T3-E1 cells. *J Bone Miner Res* 1994;9:843–854.
- Solchaga LA, Cassiede P, Caplan AI. Different response to osteo-inductive agents in bone marrow- and periosteum-derived cell preparations. *Acta Orthop Scand* 1998;69:426–432.
- de Bruijn JD, van den Brink I, Bovell YP, van Blitterswijk CA. Tissue engineering of goat bone: Osteogenic potential of goat bone marrow cells. *Bioceramics* 1998;11:497–500.
- Jaiswal N, Haynesworth SE, Caplan AI, Bruder SP. Osteogenic differentiation of purified, culture-expanded human mesenchymal stem cells in vitro. *J Cell Biochem* 1997;64:295–312.
- Purpura KA, Aubin JE, Zandstra PW. Sustained in vitro expansion of bone progenitors is cell density dependent. *Stem Cells* 2004;22:39–50.
- Both SK, van der Muijsenberg AJ, van Blitterswijk CA, de Boer J, de Bruijn JD. A rapid and efficient method for expansion of human mesenchymal stem cells. *Tissue Eng* 2007;13:3–9.
- Anselme K, Noel B, Flautre B, Blary MC, Delecourt C, Descamps M, Hardouin P. Association of porous hydroxyapatite and bone marrow cells for bone regeneration. *Bone* 1999;25(2 Suppl):51S–54S.
- Holy CE, Shoichet MS, Davies JE. Engineering three-dimensional bone tissue in vitro using biodegradable scaffolds: Investigating initial cell-seeding density and culture period. *J Biomed Mater Res* 2000;51:376–382.
- Ishaug-Riley SL, Crane-Kruger GM, Yaszemski MJ, Mikos AG. Three-dimensional culture of rat calvarial osteoblasts in porous biodegradable polymers. *Biomaterials* 1998;19:1405–1412.
- Wiedmann-Al-Ahmad M, Gutwald R, Lauer G, Hubner U, Schmelzeisen R. How to optimize seeding and culturing of human osteoblast-like cells on various biomaterials. *Biomaterials* 2002;23:3319–3328.
- Wilson CE, Dhert WJ, Van Blitterswijk CA, Verbout AJ, De Bruijn JD. Evaluating 3D bone tissue engineered constructs with different seeding densities using the alamarBlue assay and the effect on in vivo bone formation. *J Mater Sci Mater Med* 2002;13:1265–1269.
- Gloekner H, Jonuleit T, Lemke HD. Monitoring of cell viability and cell growth in a hollow-fiber bioreactor by use of the dye Alamar Blue. *J Immunol Methods* 2001;252:131–138.
- Unsworth JM, Rose FR, Wright E, Scotchford CA, Shakesheff KM. Seeding cells into needled felt scaffolds for tissue engineering applications. *J Biomed Mater Res A* 2003;66:425–431.
- Liu Y, Cooper PR, Barralet JE, Shelton RM. Influence of calcium phosphate crystal assemblies on the proliferation and osteogenic gene expression of rat bone marrow stromal cells. *Biomaterials* 2007;28:1393–1403.
- Zou X, Li H, Zou L, Mygind T, Lind M, Bunker C. Porous tantalum trabecular metal scaffolds in combination with a novel marrow processing technique to replace autograft. *Adv Exp Med Biol* 2006;585:197–208.
- Wilson CE, de Bruijn JD, van Blitterswijk CA, Verbout AJ, Dhert WJ. Design and fabrication of standardized hydroxyapatite scaffolds with a defined macro-architecture by rapid prototyping for bone-tissue-engineering research. *J Biomed Mater Res* 2004;68A:123–132.
- van Gaalen SM, Dhert WJ, van den Muysenberg A, Oner FC, van Blitterswijk C, Verbout AJ, de Bruijn JD. Bone tissue engineering for spine fusion: An experimental study on ectopic and orthotopic implants in rats. *Tissue Eng* 2004;10:231–239.
- Li S, de Wijn JR, Li J, Layrolle P, de Groot K. Macroporous biphasic calcium phosphate scaffold with high permeability/porosity ratio. *Tissue Eng* 2003;9:535–548.
- Faragher RG, Kill IR, Hunter JA, Pope FM, Tannock C, Shall S. The gene responsible for Werner syndrome may be a cell division “counting” gene. *Proc Natl Acad Sci USA* 1993;90:12030–12034.
- van der Lubbe HB, Klein CP, de Groot K. A simple method for preparing thin (10 microM) histological sections of undecalcified plastic embedded bone with implants. *Stain Technol* 1988;63:171–176.
- Kruyt MC, Dhert WJ, Yuan H, Wilson CE, van Blitterswijk CA, Verbout AJ, de Bruijn JD. Bone tissue engineering in a critical size defect compared to ectopic implantations in the goat. *J Orthop Res* 2004;22:544–551.
- Parfitt AM, Drezner MK, Glorieux FH, Kanis JA, Malluche H, Meunier PJ, Ott SM, Recker RR. Bone histomorphometry: Standardization of nomenclature, symbols, and units. Report of the ASBMR Histomorphometry Nomenclature Committee. *J Bone Miner Res* 1987;2:595–610.
- Ryoo HM, van Wijnen AJ, Stein JL, Lian JB, Stein GS. Detection of a proliferation specific gene during development of the osteoblast phenotype by mRNA differential display. *J Cell Biochem* 1997;64:106–116.